Status of Charm decays and Charm Spectroscopy.

Antimo Palano
INFN and University of Bari
PBF Workshop, Annecy, June 31, 2011

Sections involved.

- 16.1 Charmed meson decays.
- 16.3 Charmed meson spectroscopy.

- People involved:
- A. Palano, J. Brodzicka (Belle), T. Shroeder, P. Roudeau, C. Chen, F. Simonetto (experiment).
- S.Fajfer, P. Colangelo (theory).

Status of Charmed meson decays.

- Two-body decays.
- Theory section: S.Fajfer?
- **Experimental part in progress**.

- Three-body decays. **Partly written.** To be uploaded.
- Methodology in a different section.
- Dalitz analyses. Some in related to D-mixing or γ in different sections.

$D^0 \to K^-\pi^+\pi^0$, $D^0 \to \bar{K}^0\pi^+\pi^-$

- Other analyses are in this section. Mostly BaBar.

$D^0 \to \bar{K}^0 K^+ K^-$, $D^0 \to \pi^-\pi^+\pi^0$, $D^0 \to K^- K^+\pi^0$

$D_s^+ \to \pi^+\pi^-\pi^+$, $D_s^+ \to K^+K^-\pi^+$

Some text from Dalitz analyses.

□ Dalitz Plot Analysis of $D^0 \to \bar{K}^0 K^+ K$

0.1 Dalitz Analysis of three-body Charmed Mesons Decays

0.1.1 Introduction

Dalitz plot analyses of three-body charm decays can provide new information on the resonances that contribute to observed three-body final states. In addition, since the intermediate quasi-two-body modes are dominated by light quark meson resonances, new information on light meson spectroscopy can be obtained.

Puzzles still remain in light meson spectroscopy. There are new claims for the existence of broad states close to threshold such as $\kappa(800)$ and $\sigma(500)$ **?**. The new evidence has reopened discussion of the composition of the ground state $J^{PC} = 0^{++}$ nonet, and of the possibility that states such as the $a_0(980)$ or $f_0(980)$ may be 4-quark states due to their proximity to the $\bar{K}K$ threshold **?**. This hypothesis can only be tested through an accurate measurement of branching fractions and couplings to different final states. In addition, comparison between the production of these states in decays of differently flavored charmed mesons $D^0(c\bar{u})$, $D^+(c\bar{d})$ and $D_s^+(c\bar{s})$ can yield new information on their possible quark composition. Another benefit of studying charm decays is that, in some cases, partial wave analyses are able to isolate the scalar contribution almost background free.

0.1.2 Dalitz Plot Analysis of $D^0 \to \overline{K}^0 K^+ K^-$

This paper from *BABAR* focuses on the study of the three-body D^0 meson decay

$$D^0 \to \overline{K}^0 K^+ K^-,$$

where the $\overline{K}^0$ is detected via the decay $K_S^0 \to \pi^+\pi^-$. The D^0 is tagged with a D^*. *BABAR* makes use of 91.5 fb^{-1}

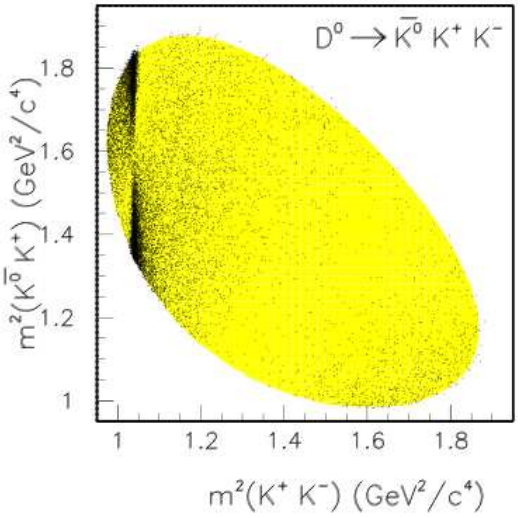

Fig. 1. Dalitz plot of $D^0 \to \overline{K}^0 K^+ K^-$.

collecting N=13536 ± 116 events with a 97.3% purity. An additional analysis, with increased statistics has been performed in the environment of D^0 mixing and it has been discussed in sect. XX. Here we focus on the Partial Wave Analysis of the K^+K^- threshold region.

The Dalitz plot for these $D^0 \to \overline{K}^0 K^+ K^-$ candidates is shown in Fig. 1.

In the K^+K^- threshold region, a strong $\phi(1020)$ signal is observed, together with a rather broad structure. A large asymmetry with respect to the $\overline{K}^0 K^+$ axis can also be seen in the vicinity of the $\phi(1020)$ signal, which is the result of interference between S and P-wave amplitude contributions to the K^+K^- system. The $f_0(980)$

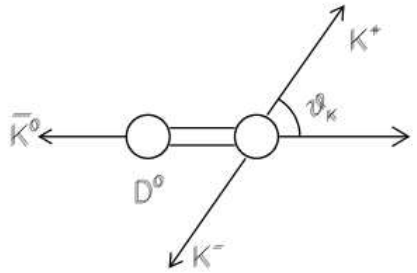

Fig. 2. The kinematics describing the production of the K^+K^- system in the threshold region of the decay $D^0 \to \overline{K}^0 K^+ K^-$.

$\overline{K}^0$) rest frame. The K^+K^- mass distribution has been modified by weighting each D^0 candidate by the spherical harmonic $Y_L^0(\cos\theta_K)$ (L=0-4) divided by its (Dalitz-plot-dependent) fitted efficiency. The resulting distributions $\langle Y_L^0 \rangle$ are shown in Fig. 3 and are proportional to the K^+K^- mass-dependent harmonic moments. It is found that all the $\langle Y_L^0 \rangle$ moments are small or consistent with zero, except for $\langle Y_0^0 \rangle$, $\langle Y_1^0 \rangle$ and $\langle Y_2^0 \rangle$.

In order to interpret these distributions a simple partial wave analysis has been performed, involving only S- and P-wave amplitudes. This results in the following set of equations **?**:

$$\sqrt{4\pi}\,\langle Y_0^0 \rangle = S^2 + P^2$$
$$\sqrt{4\pi}\,\langle Y_1^0 \rangle = 2 \mid S \mid\mid P \mid \cos\phi_{SP} \qquad (3)$$

Some text from Dalitz analyses.

- Dalitz Plot Analysis of $D_s^+ \to \bar{\pi}^+\pi^-\pi^+$.

1.05 GeV/c^2 and corrected for phase space. It is possible to observe that the two distributions show a good agreement, supporting the argument that the $f_0(980)$ contribution is small.

0.1.3 Dalitz Plot Analysis of three-body D_s^+ decays.

0.1.3.1 $D_s^+ \to \pi^+\pi^-\pi^+$

BABAR has performed a Dalitz plot analysis of $D_s^+ \to \pi^+\pi^-\pi^+$ and $D_s^+ \to K^+K^-\pi^+$ using 380 fb^{-1}. The selection of the two channels is similar and it will be described only once.

The three tracks are fitted to a common vertex, and the χ^2 fit probability (labeled P_1) must be greater than 0.1 %. A separate kinematic fit which makes use of the D_s^+ mass constraint, to be used in the Dalitz plot analysis, is also performed. To help discriminate signal from background, an additional fit which uses the constraint that the three tracks originate from the e^+e^- luminous region (beam spot) is performed. The χ^2 probability of this fit is labeled as P_2, and it is expected to be large for background and small for D_s^+ signal events, since in general the latter will have a measurable flight distance.

The combinatorial background is reduced by requiring the D_s^+ to originate from the decay

$$D_s^*(2112)^+ \to D_s^+\gamma \qquad (1)$$

using the mass difference $\Delta m = m(\pi^+\pi^-\pi^+\gamma) - m(\pi^+\pi^-\pi^+)$. Each D_s^+ candidate is characterized by three variables: the center of mass momentum p^*, the difference in probability $P_1 - P_2$, and the signed decay distance d_{xy} between the D_s^+ decay vertex and the beam spot projected in the plane normal to the beam collision axis. The distributions for these variables for background are inferred from the $D_s^+ \to \pi^+\pi^-\pi^+$ invariant mass sidebands. Since these variables are (to a good approximation) independent of the decay mode, the distributions for the three-pion invari-

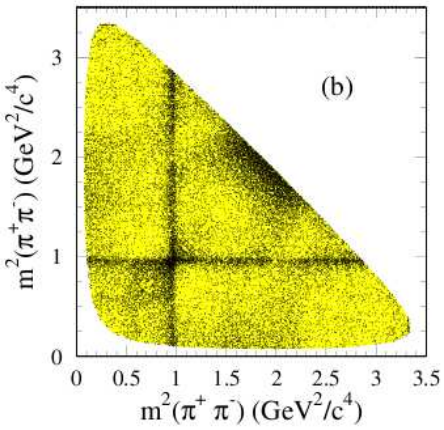

Fig. 7. Symmetrized $D_s^+ \to \pi^+\pi^-\pi^+$ Dalitz plot (two entries per event).

$m(\pi^+K^-_{\rm mis}\pi^+) - m(K^-_{\rm mis}\pi^+) < 0.1475$ GeV/c^2 diminishes this background.

The resulting D_s^+ signal region contains 13179 events with a purity of 80%. The resulting Dalitz plot, symmetrized along the two axes, is shown in Fig. 7. For this distribution, and in the following Dalitz plot analysis, the track momenta obtained from the D_s^+ mass-constrained fit are used. We observe a clear $f_0(980)$ signal, evidenced by the two narrow crossing bands. We also observe a broad accumulation of events in the 1.9 GeV^2/c^4 region. The efficiency is found to be almost uniform as a function of the $\pi^+\pi^-$ invariant mass with an average value of $\approx$ 1.6 %.

In the Dalitz plot analysis spin-1 and spin-2 resonances are described by relativistic Breit-Wigner. For the $\pi^+\pi^-$ $\mathcal{S}$-wave amplitude, a different approach is used because:

– Scalar resonances have large uncertainties. In addition, the existence of some states needs confirmation.

Status of Charmed meson decays.

- Semileptonic charm decays (in progress from P. Roudeau (BaBar)).
- Rare decays (in progress from C. Chen (BaBar))

Status of Charmed meson spectroscopy.

A first draft has been uploaded.

- **Theory section written by P. Colangelo.**
- **Today received contribution from Jolanta.**
- Work needed to syncronize the two contributions. Time sequence or focus on the different particles?
- At moment we started the description in chronological order.
- **Two sections**.
- D_J spectroscopy from B decays and $c\bar{c}$ continuum.
- D_{sJ} spectroscopy from B decays and $c\bar{c}$ continuum.

Status of Charmed meson spectroscopy.

- BaBar based text only.

Status of Charmed meson spectroscopy.

- Theory section written by P. Colangelo.

Constituent quark models

Quark models are traditionally a method to compute properties like hadron masses and couplings. In such approaches the hadrons are approximately described in terms of rest-frame valence quark configurations, the dynamics of which is governed by a Hamiltonian derived from (or inspired to) QCD. In particular, quark confinement is implemented by a flavour-independent, linearly increasing Lorentz-scalar interquark interaction at large distances, while the short-distance quark dynamics is described by a one-gluon exchange interaction. For a system comprising a heavy quark $Q = c$ and a light antiquark $\bar{q} = \bar{u}, \bar{d}, \bar{s}$, the Hamiltonian is written as Godfrey and Isgur (1985)

$$H = H_0 + V \quad , \tag{1}$$

where

$$H_0 = (p^2 + m_Q^2)^{1/2} + (p^2 + m_{\bar{q}}^2)^{1/2} \tag{2}$$

is the kinetic term, with p the modulus of the quark three-momentum in the meson rest-frame. The potential V includes spin-independent and spin-dependent terms:

$$V = V_0 + V^{hyp} + V^{so} \quad . \tag{3}$$

V_0 is the confining+Coulombic potential

$$V_0 = -\frac{4}{3}\frac{\alpha_s(r)}{r} + c + \sigma^2 r \tag{4}$$

with c and σ^2 parameters. V^{hyp} describes the spin-spin interaction

$$V^{hyp} = \frac{4}{3}\frac{\alpha_s(r)}{m_Q m_{\bar{q}}}\Big[\frac{8\pi}{3}\boldsymbol{s}_Q \cdot \boldsymbol{s}_{\bar{q}}\,\delta^3(\boldsymbol{r}) + \frac{1}{r^3}\left(3\frac{(\boldsymbol{s}_Q \cdot \boldsymbol{r})(\boldsymbol{s}_{\bar{q}} \cdot \boldsymbol{r})}{r^2} - \boldsymbol{s}_Q \cdot \boldsymbol{s}_{\bar{q}}\right)\Big] \tag{5}$$

are input parameters, and do not coincide with the ("current") masses appearing in the QCD Lagrangian. For the light u and d quarks the constituent masses are fixed to values of $\mathcal{O}(100\,MeV)$, and of $\mathcal{O}(300\,MeV)$ for the strange quark, well above the values of the current masses in the QCD Lagrangian.

- The running of the strong coupling α_s can be implemented as a dependence on the interquark distance, $\alpha_s = \alpha_s(r)$; each model is characterized by the way this property is fulfilled.
- Spin dependent terms in the potential present singularities of the type $1/r^n$ with $n > 1$, corresponding to "illegal" operators in the wave equation. This is a consequence of reducing the relativistic quark-antiquark interaction to an istantaneous potential. The treatment of such singularities requires a smearing at small distances, which introduces a model dependence in the calculation of the meson properties.
- The effect of nearby multi-hadron thresholds (or quark unquenching) is not taken into account in the calculation of, e.g., the mass spectrum. Although such an approximation is legitimate in the limit of large number of colors, in real QCD it represents a systematic uncertainty affecting, in particular, the determination of the masses of the orbital and radial excitations.

In a quark model approach the $c\bar{q}$ spectrum ($q = u, d, s$) was already computed long ago, namely in Godfrey and Isgur (1985) with results (shown in Table 1) rather close to data in the case of the lightest $s-$wave ($L = 0$) states and of two $J^P = 2^+$ and $J^P = 1^+$ $p-$wave ($L = 1$) states. As for the state with $J^P = 0^+$ and the second state with $J^P = 1^+$ (both with $L = 1$), in the $c\bar{s}$ case the predicted masses are larger (by about 100 MeV) than the masses of the scalar and axial vector D_{sJ} mesons discussed in this chapter. Several modifications and improvements have been implemented, namely in models based on the expansion of the Hamiltonian (1) in the inverse mass of the charm quark, in the spirit of the heavy quark

Status of Charmed meson spectroscopy.

- D^* mesons.

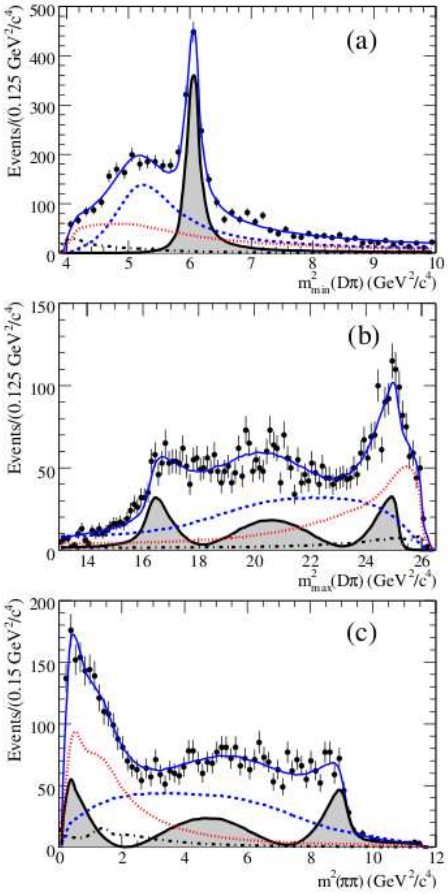

Fig. 2. Result of the fit to the data: projections on (a)

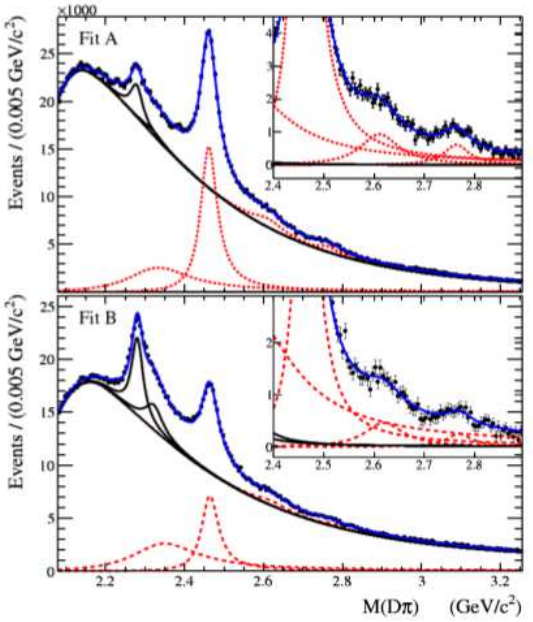

Fig. 3. Mass distribution for $D^+\pi^-$ (top) and $D^0\pi^+$ (bottom) candidates. Points correspond to data, with the total fit overlaid as a solid curve. The dotted curves are the signal components. The lower solid curves correspond to the smooth combinatoric background and to the peaking backgrounds at 2.3 GeV/c^2. The inset plots show the distributions after subtraction of the combinatoric background.

of the $D_1(2420)^+$ and $D_2^*(2460)^+$ to $D^{*0}\pi^+$ where the D^{*0} decays to $D^0\pi^0$.

– Both $D^+\pi^-$ and $D^0\pi^+$ mass distributions show new structures around 2.6 and 2.75 GeV/c^2. These enhancements are labeled as $D^*(2600)$ and $D^*(2760)$.

Status of Charmed meson spectroscopy.

- D_{sJ} mesons.

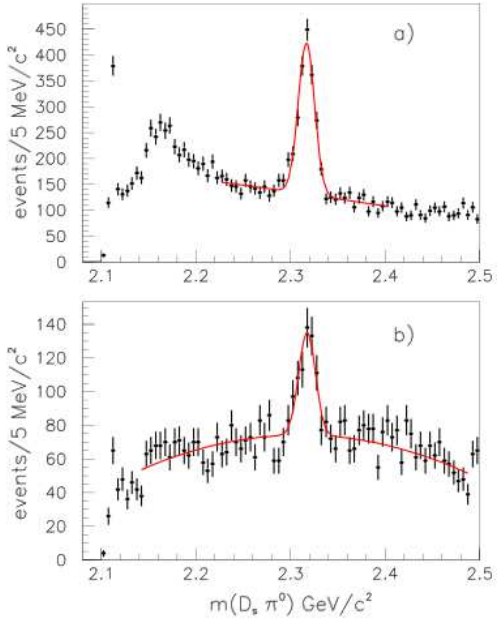

Fig. 7. a) $D_s^+\pi^0$ mass spectrum for $p^* > 3.5 GeV/c$ with superimposed the fit described in the text. The dashed line represents the estimated feedthrough from $D_{sJ}(2460)^+$. b) $D_s^+\pi^0$ mass distribution from the the decay $D_s^+ \to K^+K^-\pi^+\pi^0$. The shaded region is from D_s^+ sidebands.

where θ_h is the helicity angle. The signal-to-background ratio is further improved by requiring $|\cos\theta_h| > 0.5$.

The resulting $K^+K^-\pi^+$ mass distribution shows now a clean D_s^+ signal containing approximately 80,000 events.

Candidates in the D^+ signal region are combined with

A first fit to this spectrum is performed using a Gaussian function describing the 2.32 GeV/c^2 signal and a polynomial background. The fit yields 1267 ± 53 candidates in the signal Gaussian with mass (2316.8 ± 0.4) MeV/c^2 and standard deviation (8.6 ± 0.4) MeV/c^2.

For reasons which will become clear later, the $D_s^+\pi^0$ mass spectrum was fitted a second time to incorporate the presence of the $D_{sJ}(2460)^+$ reflection.

0.2.3 The $D_{sJ}^*(2317)^+$ from $D_s^+ \to K^+K^-\pi^+\pi^0$

As a cross check, *BABAR* selected a sample of $D_s^+ \to K^+K^-\pi^+\pi^0$ by adding π^0 candidates to each $K^+K^-\pi^+$ combination. A clear D_s^+ signal on top of a large combinatorial background is observed. Each resulting D_s^+ candidate was combined with a second π^0 candidate with laboratory momentum greater than 300 MeV/c. The "π^0 veto" request was also been applied. The center of mass momentum of the $K^+K^-\pi^+\pi^0\pi^0$ system was required to be greater that 3.5 GeV/c.

The resulting $D_s^+\pi^0$ mass distribution is shown in fig. 7b) where a clear $D_{sJ}^*(2317)^+$ signal is observed. A Gaussian fit yields 273 ± 33 events with a mean of (2317.6 ± 1.3) MeV/c^2 and width (8.8 ± 1.1) MeV/c^2. The mean and width are consistent with the values obtained for the $D_s^+ \to K^+K^-\pi^+$ decay mode confirming unambiguously the existence of the new state.

Monte Carlo simulations were used to investigate the possibility that the $D_{sJ}^*(2317)^+$ signal could be due to reflection from other charmed states. This simulation included $e^+e^- \to c\bar{c}$ events and all known charm states and decays. The generated events were processed by a detailed detector simulation and subjected to the same reconstruction and event-selection procedure as that used for the data. No peak was found in the 2.32 GeV/c^2 $D_s^+\pi^0$ signal region.

0.3 Study of the $D_s^+\pi^0\gamma$ system and the observation of $D_{sJ}(2460)^+$.

Status of Charmed meson spectroscopy.

- D_{sJ} mesons.

DDK observes a new spin-1 resonance decaying to DK: $D^*_{s1}(2710)^+$.

0.8 Belle B decay goes here?

0.8.1 Inclusive study of the DK system.

The *BABAR* study is performd inclusively, with the DK and D^*K systems separated from the $B\bar{B}$ background by means of the center of mass momentum $p^* > 3.5$ GeV/c. Neutral D^0 mesons are reconstructed as $D^0 \to K^-\pi^+$ while D^+ are reconstructed as $D^+ \to K^-\pi^+\pi^+$. Kaons are reconstructed in the charged and neutral modes.

To improve the signal to background ratio a study is performed of the distribution of θ_{K^+} ($\theta_{K^0_S}$), the angle between the K^+ (K^0_S) direction in the DK rest frame and the DK direction in the laboratory frame. The distribution of this angle is expected to be symmetric around zero, but an accumulation of combinatorial background close to $\cos\theta_K = -1$ is observed. Due to the jetlike nature of the reaction $e^+e^- \to c\bar{c}$ this background is interpreted as due to combinations for which the K comes from the jet opposite to the D meson. A conservative cut requiring $\cos\theta_K > -0.8$ is applied to the data.

To improve the mass resolution, the nominal D mass and the reconstructed 3-momentum are used to calculate the D energy. The sideband-subtracted D^0K^+ and $D^+K^0_S$ mass spectra are shown in Fig. 15(a) and Fig. 15(c). The two mass spectra in Fig. 15 present similar features. The single bin peak at 2.4 GeV/c^2 results from decays of $D_{s1}(2536)^+$ to $D^{*0}K^+$ or $D^{*+}K^0_S$ in which the π^0 or γ from the D^* decay is missed. Since the $D_{s1}(2536)^+$ is believed to have $J^P = 1^+$, decay to DK is forbidden by angular momentum and parity conservation. The spectrum shows a prominent narrow signal due to the

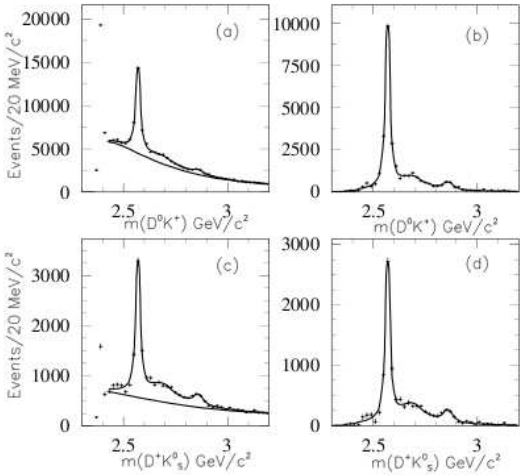

Fig. 15. Sideband-subtracted DK invariant mass distributions for (a) $D^0_{K^-\pi^+}K^+$, (c) $D^+_{K^-\pi^+\pi^+}K^0_s$; (b) and (d) show the fitted-background-subtracted mass spectra.

Table 5. The χ^2/NDF and resonance parameter values obtained from the fits to the DK and D^*K mass spectra. Masses and widths are given in units of MeV/c^2 and MeV, respectively. Uncertainties are statistical only.

System	χ^2/NDF	$D^*_{s1}(2710)^+$	$D^*_{sJ}(2860)^+$	$D_{sJ}(3040)^+$
DK	85/56	$m = 2710.0 \pm 3.3$ $\Gamma = 178 \pm 19$	$m = 2860.0 \pm 2.3$ $\Gamma = 53 \pm 6$	
D^*K	51/33	$m = 2712 \pm 3$ $\Gamma = 103 \pm 8$	$m = 2865.2 \pm 3.5$ $\Gamma = 44 \pm 8.3$	$m = 3042 \pm 9$ $\Gamma = 214 \pm 34$